

Non-Markovian dynamics in a spin star system: Exact solution and approximation techniques

Heinz-Peter Breuer,¹ Daniel Burgarth,¹ and Francesco Petruccione^{1,2}

¹*Physikalisches Institut, Universität Freiburg, Hermann-Herder-Str. 3, D-79104 Freiburg, Germany*

²*School of Pure and Applied Physics, University of KwaZulu-Natal, 4041 Durban, South Africa*

(Received 9 January 2004; published 30 July 2004)

The reduced dynamics of a central spin coupled to a bath of N spin- $\frac{1}{2}$ particles arranged in a spin star configuration is investigated. The exact time evolution of the reduced density operator is derived, and an analytical solution is obtained in the limit $N \rightarrow \infty$ of an infinite number of bath spins, where the model shows complete relaxation and partial decoherence. It is demonstrated that the dynamics of the central spin cannot be treated within the Born-Markov approximation. The Nakajima-Zwanzig and the time-convolutionless projection operator technique are applied to the spin star system. The performance of the corresponding perturbation expansions of the non-Markovian equations of motion is examined through a comparison with the exact solution.

DOI: 10.1103/PhysRevB.70.045323

PACS number(s): 73.21.La, 03.65.Yz, 05.30.-d, 75.10.Jm

I. INTRODUCTION

Solid state spin nanodevices are known as very promising candidates for quantum computation¹⁻⁴ and also for quantum communication.⁵ They provide a scalable system that can easily be integrated into standard silicon technology. A drawback of such systems compared to other proposals for quantum computing, such as ion traps⁶ and cavity QED,⁷ are the many degrees of freedom of the surrounding material causing dissipation and decoherence.⁸ The first step in overcoming these disadvantages is to be able to model them.

An important contribution to quantum noise in solid state systems arises from the nuclear spins, and recently much work has been devoted to the modeling of spin bath systems⁹⁻¹⁷ (for a review, see Refs. 18 and 19). The interaction of a central spin with a bath of environmental spins often leads to strong non-Markovian behavior. The usual derivations of Markovian quantum master equations known, e.g., from atomic physics²⁰ and quantum optics²¹ therefore fail for many spin bath models, and a detailed investigation of methods is required that are capable of going beyond the Markovian approximation.

In this paper, we examine the reduced dynamics of a simple spin star system. The advantage of this model is that, while showing several interesting features such as partial decoherence and strong non-Markovian behavior, it is exactly solvable due to its high symmetry. The model therefore represents an appropriate example for a general discussion of the performance of various non-Markovian methods. We study here the Nakajima-Zwanzig²²⁻²⁴ and the time-convolutionless projection operator technique²⁵⁻²⁸ and derive and analyze the perturbation expansions of the corresponding non-Markovian master equations.

The paper is organized as follows. In Sec. II, we introduce the model investigated, a spin star model involving a Heisenberg XY coupling (Sec. II A), and determine the exact time evolution of the central spin (Sec. II B). In Sec. II C we analyze the limit of an infinite number of bath spins, discuss the behavior of the von Neumann entropy of the central spin, and demonstrate that the model exhibits complete relaxation and partial decoherence. Several non-Markovian approxima-

tion techniques are discussed in Sec. III. The dynamic equations found in second order in the coupling are introduced in Sec. III A, where it is also demonstrated that the prominent Born-Markov approximation is not applicable to the spin star model. Employing a technique that enables the calculation of the correlation functions of the spin bath, we derive in Sec. III B the perturbation expansions corresponding to the Nakajima-Zwanzig and to the time-convolutionless projection operator technique and compare these approximations with the analytical solution for the dynamics of the central spin. Finally, the conclusions are drawn in Sec. IV.

II. EXACT DYNAMICS

A. The model

We consider a “spin star” configuration,²⁹ which consists of $N+1$ localized spin- $\frac{1}{2}$ particles. One of the spins is located at the center of the star, while the other spins, labeled by an index $i=1, 2, \dots, N$, surround the central spin at equal distances on a sphere. In the language of open quantum systems⁸ we regard the central spin with Pauli spin operator $\boldsymbol{\sigma}$ as an open system “living” in a two-dimensional Hilbert space \mathcal{H}_S and the surrounding spins described by the spin operators $\boldsymbol{\sigma}^{(i)}$ as a spin bath with Hilbert space \mathcal{H}_B , which is given by an N -fold tensor product of two dimensional spaces.

The central spin $\boldsymbol{\sigma}$ interacts with the bath spins $\boldsymbol{\sigma}^{(i)}$ via a Heisenberg XY interaction³⁰ represented through the Hamiltonian

$$\alpha H = 2\alpha(\sigma_+ J_- + \sigma_- J_+), \quad (1)$$

where

$$J_{\pm} \equiv \sum_{i=1}^N \sigma_{\pm}^{(i)}, \quad (2)$$

and

$$\sigma_{\pm}^{(i)} \equiv \frac{1}{2}(\sigma_1^{(i)} \pm i\sigma_2^{(i)}) \quad (3)$$

represents the raising and lowering operators of the i th bath spin. The Heisenberg XY coupling has been found to be an effective Hamiltonian in many physical systems such as quantum dots,³¹ cavity QED,³² two-dimensional electron gases,³³ and optical lattices.³⁴ Equation (1) describes a very simple time-independent interaction with equal coupling strength α for all bath spins. It is invariant under rotations around the z axis. The operator $\mathbf{J} \equiv 1/2 \sum_{i=1}^N \boldsymbol{\sigma}^{(i)}$ represents the total spin angular momentum of the bath (units are chosen such that $\hbar=1$). The central spin thus couples to the collective bath angular momentum.

We introduce an orthonormal basis in the bath Hilbert space \mathcal{H}_B consisting of states $|j, m, \nu\rangle$. These states are defined as eigenstates of J_3 (eigenvalue m) and of \mathbf{J}^2 [eigenvalue $j(j+1)$]. The index ν labels the different eigenstates in the eigenspace $\mathcal{M}_{j,m}$ belonging to a given pair (j, m) of quantum numbers. As usual, $j \leq N/2$ and $-j \leq m \leq j$. The dimension of $\mathcal{M}_{j,m}$ is given by the expression^{29,35}

$$n(j, N) = \binom{N}{N/2-j} - \binom{N}{N/2-j-1}. \quad (4)$$

We further introduce the usual superoperator notation for the Liouville operator

$$\mathcal{L}\rho(t) \equiv -i[H, \rho(t)], \quad (5)$$

where $\rho(t)$ denotes the density matrix of the total system in the Hilbert space $\mathcal{H}_S \otimes \mathcal{H}_B$. The formal solution of the von Neumann equation

$$\frac{d}{dt}\rho(t) = \alpha\mathcal{L}\rho(t) \quad (6)$$

can then be written as

$$\rho(t) = \exp(\alpha\mathcal{L}t)\rho(0). \quad (7)$$

Our main goal is to derive the dynamics of the reduced density matrix

$$\rho_S(t) \equiv \text{tr}_B\{\rho(t)\}, \quad (8)$$

where tr_B denotes the partial trace taken over the Hilbert space \mathcal{H}_B of the spin bath. The reduced density matrix is completely determined in terms of the Bloch vector

$$\mathbf{v}(t) = \begin{pmatrix} v_1(t) \\ v_2(t) \\ v_3(t) \end{pmatrix} \equiv \text{tr}_S\{\boldsymbol{\sigma}\rho_S(t)\} \quad (9)$$

through the relationship

$$\rho_S(t) = \frac{1}{2} \begin{pmatrix} 1 + v_3(t) & v_1(t) - iv_2(t) \\ v_1(t) + iv_2(t) & 1 - v_3(t) \end{pmatrix}, \quad (10)$$

where tr_S denotes the partial trace over the Hilbert space \mathcal{H}_S of the central spin. We note that the length $r(t) \equiv |\mathbf{v}(t)|$ of the Bloch vector is equal to 1 if and only if $\rho_S(t)$ describes a pure state, and that the von Neumann entropy S of the central spin

can be expressed as a function of the length $r(t)$ of the Bloch vector:

$$\begin{aligned} S &\equiv \text{tr}_S\{-\rho_S \ln \rho_S\} \\ &= \ln 2 - \frac{1}{2}(1-r)\ln(1-r) + \frac{1}{2}(1+r)\ln(1+r). \end{aligned} \quad (11)$$

The initial state of the reduced system at $t=0$ is taken to be an arbitrary (possibly mixed) state

$$\rho_S(0) = \begin{pmatrix} \frac{1+v_3(0)}{2} & v_-(0) \\ v_+(0) & \frac{1-v_3(0)}{2} \end{pmatrix}, \quad (12)$$

while the spin bath is assumed to be in an unpolarized infinite temperature state:

$$\rho_B(0) = 2^{-N}I_B. \quad (13)$$

Here, I_B denotes the unit matrix in \mathcal{H}_B , and we have defined the v_{\pm} as linear combinations of the components $v_{1,2}$ of the Bloch vector:

$$v_{\pm} = \frac{v_1 \pm iv_2}{2}. \quad (14)$$

The initial state of the total system is given by an uncorrelated product state $\rho_S(0) \otimes \rho_B(0)$.

B. Reduced system dynamics

In this section, we will derive the exact dynamics of the reduced density matrix $\rho_S(t)$ for the model given above. One possibility of obtaining the evolution of the central spin is to substitute Eq. (7) into Eq. (8) and to expand the exponential with respect to the coupling. This yields

$$\begin{aligned} \rho_S(t) &\equiv \text{tr}_B\{\exp(\alpha\mathcal{L}t)\rho_S(0) \otimes \rho_B(0)\} \\ &= \sum_{k=0}^{\infty} \frac{(\alpha t)^k}{k!} \text{tr}_B\{\mathcal{L}^k \rho_S(0) \otimes 2^{-N}I_B\}. \end{aligned} \quad (15)$$

It is easy to verify that we have

$$H^{2n} = 4^n [\sigma_+ \sigma_- (J_- J_+)^n + \sigma_- \sigma_+ (J_+ J_-)^n] \quad (16)$$

and

$$H^{2n+1} = 2 \cdot 4^n [\sigma_+ \sigma_- (J_+ J_-)^n + \sigma_- \sigma_+ (J_- J_+)^n]. \quad (17)$$

We note that such simple expressions are obtained since a term $\sigma_3 J_3$ is missing in the interaction Hamiltonian. We substitute the last two equations into

$$\mathcal{L}^n \rho = i^n \sum_{k=0}^n (-1)^k \binom{n}{k} H^k \rho H^{n-k} \quad (18)$$

to get the formulas

$$\text{tr}_B\{\mathcal{L}^{2k-1} \rho_S(0) \otimes 2^{-N}I_B\} = 0 \quad (19)$$

and

$$\begin{aligned} & \text{tr}_B\{\mathcal{L}^{2k}\rho_S(0) \otimes 2^{-N}I_B\} \\ &= (-16)^k Q_k \frac{v_3(0)}{2} \sigma_3 + (-4)^k \left[\sum_{l=0}^k \binom{2k}{2l} R_l^{k-l} \right] \\ & \quad \times [v_-(0)\sigma_+ + v_+(0)\sigma_-], \end{aligned} \quad (20)$$

which hold for all $k=1,2,\dots$. Here, we have introduced the bath correlation functions

$$Q_k \equiv \frac{1}{2^N} \text{tr}_B\{(J_+J_-)^k\}, \quad (21)$$

$$R_l^{k-l} \equiv \frac{1}{2^N} \text{tr}_B\{(J_+J_-)^{k-l}(J_-J_+)^l\}. \quad (22)$$

We will come back to these correlation functions when we discuss approximation techniques in Sec. III.

Using the formulas (19) and (20) in Eq. (15) we can express the components of the Bloch vector as follows,

$$v_{\pm}(t) = f_{12}(t)v_{\pm}(0), \quad (23)$$

$$v_3(t) = f_3(t)v_3(0), \quad (24)$$

where we have introduced the functions

$$f_{12}(t) \equiv 2^{-N} \text{tr}_B\{\cos[2\sqrt{J_+J_-}\alpha t]\cos[2\sqrt{J_-J_+}\alpha t]\}, \quad (25)$$

and

$$f_3(t) \equiv 2^{-N} \text{tr}_B\{\cos[4\sqrt{J_+J_-}\alpha t]\}. \quad (26)$$

Calculating the traces over the spin bath in the eigenbasis of J_3 and \mathbf{J}^2 using

$$J_{\mp}J_{\pm}|j,m,\nu\rangle = (j \mp m)(j \pm m + 1)|j,m,\nu\rangle, \quad (27)$$

we find

$$f_{12}(t) \equiv \sum_{j,m} n(j,N) \frac{\cos[2h(j,m)\alpha t]\cos[2h(j,-m)\alpha t]}{2^N} \quad (28)$$

and

$$f_3(t) \equiv \sum_{j,m} n(j,N) \frac{\cos[4h(j,m)\alpha t]}{2^N}, \quad (29)$$

where we have introduced the quantity $h(j,m) \equiv \sqrt{(j+m)(j-m+1)}$.

Thus we have determined the exact dynamics of the reduced system: The density matrix $\rho_S(t)$ of the central spin is given through the components of the Bloch vector, which are provided by the relations (23), (24), (28), and (29). We note that the dynamics can be expressed completely through only two real-valued functions $f_{12}(t)$ and $f_3(t)$. This fact is connected to the rotational symmetry of the system.

The reduced system dynamics has been obtained above with the help of an expansion of $\exp(\alpha\mathcal{L}t)$ with respect to the coupling constant α . It should be clear that, alternatively, the behavior of the central spin may be found directly from the solution of the Schrödinger equation for the composite sys-

tem. This solution can easily be constructed by making use of the fact that the subspaces spanned by the states $|+\rangle \otimes |j,m,\nu\rangle$ and $|-\rangle \otimes |j,m+1,\nu\rangle$ are invariant under the time evolution, where $|\pm\rangle$ denotes the eigenstate of σ_3 belonging to the eigenvalue ± 1 .

Sometimes it is useful to express the reduced dynamics in terms of superoperators instead of the Bloch vector. To this end, we introduce superoperators \mathcal{S}_{\pm} and \mathcal{S}_3 , which are defined by their action on an arbitrary operator A :

$$\mathcal{S}_{\pm}A \equiv \sigma_{\pm}A\sigma_{\mp} - \frac{1}{2}\{\sigma_{\mp}\sigma_{\pm},A\}, \quad (30)$$

$$\mathcal{S}_3A \equiv \sigma_3A\sigma_3 - A. \quad (31)$$

With these definitions we may write the reduced density matrix as follows,

$$\rho_S(t) = \frac{I_S}{2} + \frac{1}{2} \left[\left(\frac{1}{2}f_3(t) - f_{12}(t) \right) \mathcal{S}_3 - f_3(t)(\mathcal{S}_+ + \mathcal{S}_-) \right] \rho_S(0), \quad (32)$$

where I_S denotes the unit matrix in \mathcal{H}_S . Due to the nonunitary behavior of the reduced system, the superoperator on the right-hand side is not invertible for all times. This point will become important later on when we discuss approximation strategies.

C. The limit of an infinite number of bath spins

The explicit solution constructed in the previous section takes on a relatively simple form in the limit $N \rightarrow \infty$ of an infinite number of bath spins. It is demonstrated in the Appendix that for large N the bath correlation functions approach the asymptotic expression

$$Q_k \approx R_l^{k-l} \approx \frac{k!}{2^k N^k}. \quad (33)$$

Consequently, in Eq. (15) a term of the order N^k always occurs together with a factor of α^{2k} . A nontrivial finite limit $N \rightarrow \infty$ therefore exists if we rescale the coupling constant as follows,

$$\alpha \rightarrow \frac{\alpha}{\sqrt{N}}. \quad (34)$$

Using this approximation in Eq. (20) one obtains

$$\begin{aligned} & \text{tr}_B\{\mathcal{L}^{2k}\rho_S(0) \otimes 2^{-N}I_B\} \\ & \approx \frac{(-8N)^k k!}{2} [v_3(0)\sigma_3 + v_-(0)\sigma_+ + v_+(0)\sigma_-]. \end{aligned} \quad (35)$$

If we insert this into Eq. (15) we get an infinite series which yields the following expressions for the functions $f_{12}(t)$ and $f_3(t)$:

$$f_{12}(t) = 1 + g(t), \quad f_3(t) = 1 + 2g(t), \quad (36)$$

where

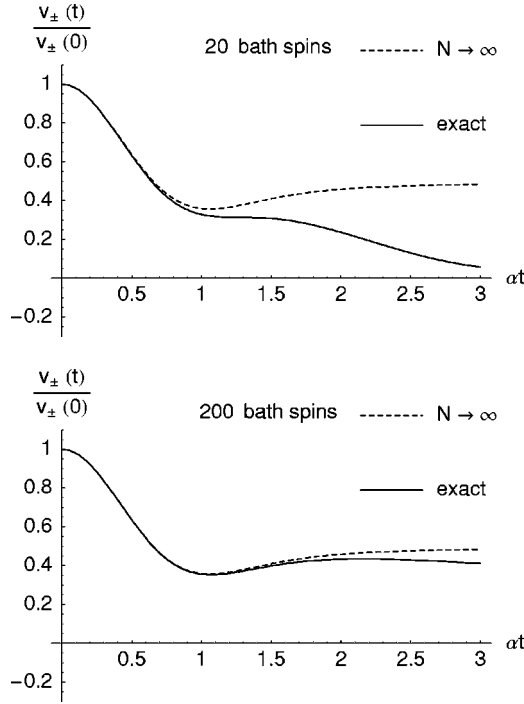


FIG. 1. Comparison of the limit $N \rightarrow \infty$ [see Eqs. (36) and (37)] with the exact functions for $N=20$ and $N=200$. The plot shows the v_{\pm} component of the Bloch vector.

$$g(t) \equiv -at \exp(-2\alpha^2 t^2) \sqrt{\frac{\pi}{2}} \operatorname{erfi}(\sqrt{2}at). \quad (37)$$

Note that $\operatorname{erfi}(x)$ is the imaginary error function. It is a real-valued function defined by

$$\operatorname{erfi}(x) \equiv \frac{\operatorname{erf}(ix)}{i}, \quad (38)$$

which leads to the Taylor series

$$\operatorname{erfi}(x) = \frac{2}{\sqrt{\pi}} \sum_{k=0}^{\infty} \frac{x^{2k+1}}{k!(2k+1)}. \quad (39)$$

Figures 1 and 2 show that this approximation obtained in the limit of an infinite number of bath spins is already reasonable for $N \approx 200$.

By contrast to $\operatorname{erf}(x)$, the imaginary error function is not bounded. However, $g(t)$ is bounded, and in the limit $t \rightarrow \infty$ we have $g(t) \rightarrow -1/2$. Thus, in this limit the system is described by the stationary density matrix

$$\lim_{t \rightarrow \infty} \lim_{N \rightarrow \infty} \rho_S(t) = \begin{pmatrix} \frac{1}{2} & \frac{v_-(0)}{2} \\ \frac{v_+(0)}{2} & \frac{1}{2} \end{pmatrix}. \quad (40)$$

The three-component of the Bloch vector relaxes to zero, while the off-diagonal elements of the density matrix show partial decoherence, i.e., they assume half of their original values. This behavior is also reflected in the von Neumann entropy of the reduced system. Its dynamics depends on the

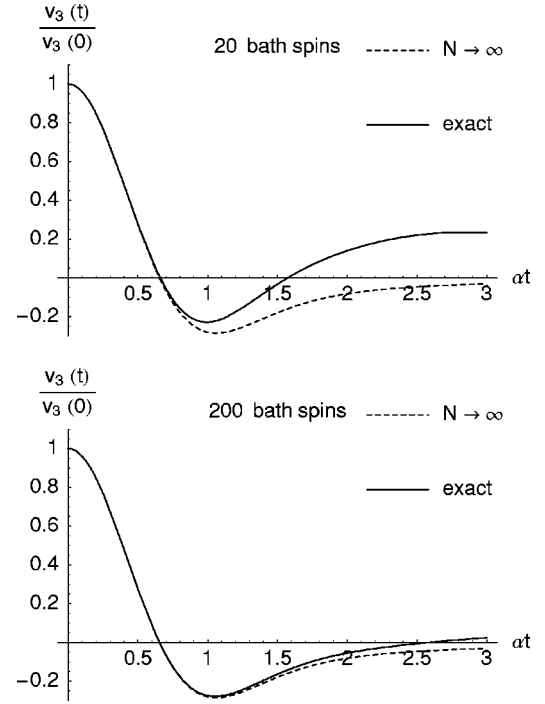


FIG. 2. Comparison of the limit $N \rightarrow \infty$ [see Eqs. (36) and (37)] with the exact functions for $N=20$ and $N=200$. The figure shows the v_3 -component of the Bloch vector.

initial entropy parametrized by $r(0)$ and on $v_3(0)$, which is obvious because the entropy is a scalar quantity and the system is invariant under rotations around the z axis. Figure 3 shows the entropy as a function of time for different initial conditions.

We remark that the solution for the dynamics of the central spin in the limit $N \rightarrow \infty$, as given by Eqs. (36) and (37), can also be found with the help of a mean field-type approximation.³⁶ To this end one introduces the scaled bath operators \mathbf{J}/\sqrt{N} into the Heisenberg equations of motion of the total system and performs the limit $N \rightarrow \infty$. As shown in the Appendix, this limit exists in the sense that all moments of the scaled bath operators in the unpolarized bath state approach a well-defined finite limit. For an unpolarized bath state the scaled bath operators can then be regarded as con-

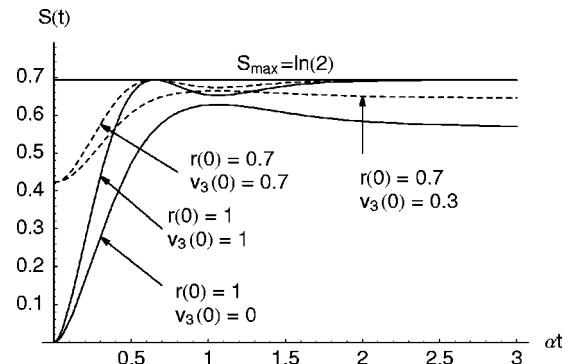


FIG. 3. von Neumann entropy $S(t)$ of the reduced system for different initial conditions in the limit $N \rightarrow \infty$. $S_{\max} \equiv \ln 2$ is the maximal entropy for a qubit, representing a completely mixed state.

stant and commuting quantities. The procedure leads to a simple set of equations of motion which are independent of N and from which one can easily determine the Bloch vector of the central spin by use of the formulae given in the Appendix.

III. APPROXIMATION TECHNIQUES

In this section we will apply different approximation techniques to the spin star model introduced and discussed in the preceding section. Due to the simplicity of this model we can not only integrate exactly the reduced system dynamics, but also construct explicitly the various master equations for the density matrix of the central spin and analyze and compare their perturbation expansions. In the following discussion we will stick to the Bloch vector notation. Each of the master equations obtained can easily be transformed into an equation involving Lindblad superoperators [see Eqs. (30) and (31)] using the translation rules

$$v_3\sigma_3 = \left\{ \frac{1}{2}\mathcal{S}_3 - \mathcal{S}_+ - \mathcal{S}_- \right\} \rho_S, \quad (41)$$

$$v_+\sigma_- + v_-\sigma_+ = -\frac{1}{2}\mathcal{S}_3\rho_S. \quad (42)$$

A. Second-order approximations

The second order approximation of the master equation for the reduced system is usually obtained within the Born approximation.⁸ It is equivalent to the second order of the Nakajima-Zwanzig projection operator technique, which will be discussed systematically in Sec. III B. In our model the Born approximation leads to the master equation

$$\begin{aligned} \dot{\rho}_S(t) &= - \int_0^t d\text{str}_B \{ [H, [H, \rho_S(s) \otimes \rho_B(0)]] \} \\ &= - 8\alpha^2 Q_1 \int_0^t ds [v_+(s)\sigma_- + v_-(s)\sigma_+ + v_3(s)\sigma_3], \end{aligned} \quad (43)$$

where the bath correlation function is found to be

$$\begin{aligned} Q_1 &= \frac{1}{2^N} \text{tr}_B \{ J_+ J_- \} = \frac{1}{2^N} \text{tr}_B \left\{ \sum_{i,j} \sigma_+^{(i)} \sigma_-^{(j)} \right\} \\ &= \frac{1}{2^N} \text{tr}_B \left\{ \sum_i \sigma_+^{(i)} \sigma_-^{(i)} \right\} = \frac{N}{2}. \end{aligned} \quad (44)$$

It is important to notice that Q_1 , as well as all other bath correlation functions are independent of time. This is to be contrasted to those situation in which the bath correlation functions decay rapidly and which therefore allow the derivation of a Markovian master equation. The time independence of the correlation functions is the main reason for the non-Markovian behavior of the spin bath model.

The integrodifferential equation (43) can easily be solved by a Laplace transformation with the solution

$$\frac{v_{\pm}(t)}{v_{\pm}(0)} = \cos(2\sqrt{N}\alpha t), \quad (45)$$

$$\frac{v_3(t)}{v_3(0)} = \cos(2\sqrt{2N}\alpha t). \quad (46)$$

In many physical applications the integration of the integrodifferential equation is much more complicated and one tries to approximate the dynamics through a master equation which is local in time. To this end, the terms $v_{\pm}(s)$ and $v_3(s)$ under the integral in Eq. (43) are replaced by $v_{\pm}(t)$ and $v_3(t)$, respectively. We thus arrive at the time local master equation

$$\begin{aligned} \frac{d}{dt} \rho_S(t) &= - 4N\alpha^2 \int_0^t ds [v_+(t)\sigma_- + v_-(t)\sigma_+ + v_3(t)\sigma_3] \\ &= - 4Nt\alpha^2 [v_+(t)\sigma_- + v_-(t)\sigma_+ + v_3(t)\sigma_3], \end{aligned} \quad (47)$$

which is sometimes referred to as Redfield equation. Also this master equation is easily solved to give the expressions

$$\frac{v_{\pm}(t)}{v_{\pm}(0)} = \exp(-2N\alpha^2 t^2), \quad (48)$$

$$\frac{v_3(t)}{v_3(0)} = \exp(-4N\alpha^2 t^2). \quad (49)$$

The Redfield equation is equivalent to the second order of the time-convolutionless projection operator technique, which will also be discussed in detail in Sec. III B.

In order to obtain, finally, a Markovian master equation, i.e., a time local equation involving a time-independent generator, one pushes the upper limit of the integral in Eq. (47) to infinity, that is one studies the limit $t \rightarrow \infty$ of the master equation. This limit leads to the Born-Markov approximation of the reduced dynamics. In the present model, however, it is not possible to perform this approximation because the integrand does not vanish for large t . Thus, the Born-Markov limit does not exist for the spin bath model investigated here and the description of relaxation and decoherence processes requires the usage of non-Markovian methods.

B. Higher-order approximations

A systematic approach to obtain approximate non-Markovian master equation in any desired order is provided by the projection operator techniques. We define a projection superoperator \mathcal{P} through the relation

$$\mathcal{P}\rho = \text{tr}_B \{ \rho \} \otimes \rho_B \quad (50)$$

with the reference state $\rho_B \equiv \rho_B(0)$ and introduce the notation

$$\langle \mathcal{X} \rangle \equiv \mathcal{P}\mathcal{X}\mathcal{P} \quad (51)$$

for any superoperator \mathcal{X} . Note that the ‘‘moments’’ $\langle \mathcal{X}^n \rangle$ are operators in the total Hilbert space $\mathcal{H}_S \otimes \mathcal{H}_B$ of the combined system.

There are two main projection operator methods: The Nakajima-Zwanzig (NZ) technique and the time-convolutionless (TCL) technique. In our model, the initial

conditions factorize. The NZ and the TCL method therefore lead to relatively simple, homogeneous equations of motion. The NZ master equation is an integrodifferential equation for the reduced density matrix with a memory $\mathcal{N}(t, \tau)$, which takes the form

$$\dot{\rho}_S(t) \otimes \rho_B = \int_0^t d\tau \mathcal{N}(t, \tau) \rho_S(\tau) \otimes \rho_B, \quad (52)$$

while the TCL master equation is a time-local equation of motion with a time-dependent generator $\mathcal{K}(t)$, which reads

$$\dot{\rho}_S(t) \otimes \rho_B = \mathcal{K}(t) \rho_S(t) \otimes \rho_B. \quad (53)$$

Both the NZ and the TCL master equation can of course be expanded with respect to the coupling strength α . Since the interaction Hamiltonian is time independent, this expansion yields

$$\int_0^t d\tau \mathcal{N}(t, \tau) \rho_S(\tau) = \sum_{n=1}^{\infty} \alpha^n \mathcal{I}_n(t, \tau) \langle \mathcal{L}^n \rangle_{pc} \rho_S(\tau) \quad (54)$$

for the NZ master equation, and

$$\mathcal{K}(t) = \sum_{n=1}^{\infty} \alpha^n \frac{t^{n-1}}{(n-1)!} \langle \mathcal{L}^n \rangle_{oc} \quad (55)$$

for the TCL master equation, where we have introduced the integral operator

$$\mathcal{I}_n(t, \tau) \equiv \int_0^t dt_1 \int_0^{t_1} dt_2 \cdots \int_0^{t_{n-3}} dt_{n-2} \int_0^{t_{n-2}} d\tau \quad (56)$$

for the ease of notion. The symbol $\langle \mathcal{L}^n \rangle_{pc}$ denotes the partial cumulants and $\langle \mathcal{L}^n \rangle_{oc}$ the ordered cumulants of order n . Their definitions can be found in Refs. 25–28. In our model we have

$$\langle \mathcal{L}^{2n+1} \rangle_{pc} = \langle \mathcal{L}^{2n+1} \rangle_{oc} = 0$$

and

$$\langle \mathcal{L}^2 \rangle_{pc} = \langle \mathcal{L}^2 \rangle,$$

$$\langle \mathcal{L}^2 \rangle_{oc} = \langle \mathcal{L}^2 \rangle,$$

$$\langle \mathcal{L}^4 \rangle_{pc} = \langle \mathcal{L}^4 \rangle - \langle \mathcal{L}^2 \rangle^2,$$

$$\langle \mathcal{L}^4 \rangle_{oc} = \langle \mathcal{L}^4 \rangle - 3\langle \mathcal{L}^2 \rangle^2,$$

$$\langle \mathcal{L}^6 \rangle_{pc} = \langle \mathcal{L}^6 \rangle - 2\langle \mathcal{L}^2 \rangle \langle \mathcal{L}^4 \rangle + \langle \mathcal{L}^2 \rangle^3,$$

$$\langle \mathcal{L}^6 \rangle_{oc} = \langle \mathcal{L}^6 \rangle - 15\langle \mathcal{L}^2 \rangle \langle \mathcal{L}^4 \rangle + 30\langle \mathcal{L}^2 \rangle^3,$$

...

In the time-independent case the ordered cumulants are just the ordinary cumulants known from classical statistics. To calculate these functions one can again use Eq. (20). The functions Q_k and R_l^{k-l} are real polynomials in N of order k . A method of determining these polynomials is sketched in the Appendix.

If we express the resulting master equations in terms of $v_{\pm}(t)$ and $v_3(t)$, we get for the TCL technique,

$$\dot{v}_{\pm}(t) = \left(\sum_{n=1}^{\infty} \alpha^{2n} \frac{s_{2n} t^{2n-1}}{(2n-1)!} \right) v_{\pm}(t), \quad (57)$$

$$\dot{v}_3(t) = \left(\sum_{n=1}^{\infty} \alpha^{2n} \frac{2q_{2n} t^{2n-1}}{(2n-1)!} \right) v_3(t), \quad (58)$$

and for the NZ method,

$$\dot{v}_{\pm}(t) = \left(\sum_{n=1}^{\infty} \alpha^{2n} \tilde{s}_{2n} \mathcal{I}_n(t, \tau) \right) v_{\pm}(\tau), \quad (59)$$

$$\dot{v}_3(t) = \left(\sum_{n=1}^{\infty} \alpha^{2n} 2\tilde{q}_{2n} \mathcal{I}_n(t, \tau) \right) v_3(\tau). \quad (60)$$

The quantities s_{2n} , \tilde{s}_{2n} , q_{2n} , and \tilde{q}_{2n} represent real polynomials in N of the order n . For example, we have

$$q_2 = -4N, \quad q_4 = -32N^2,$$

$$q_6 = -1024N + 1536N^2 - 1536N^3,$$

...

$$\tilde{q}_2 = -4N, \quad \tilde{q}_4 = 32N^2,$$

$$\tilde{q}_6 = -1024N + 1536N^2 - 1280N^3,$$

...

$$s_2 = -4N, \quad s_4 = -48N + 16N^2,$$

$$s_6 = -1024N - 384N^2 + 384N^3,$$

...

$$\tilde{s}_2 = -4N, \quad \tilde{s}_4 = -48N + 48N^2,$$

$$\tilde{s}_6 = -1024N + 2112N^2 - 1216N^3,$$

...

The $(2n)$ th-order approximation of the master equations (denoted by TCL $2n$ and NZ $2n$, respectively) is obtained by truncating the sums in Eqs. (57) and (58) and in Eqs. (59) and (60) after the n th term. In the TCL case, the resulting ordinary differential equations can be integrated very easily. The equation of motion of the NZ method can be solved with the help of a Laplace transformation. However, it may be very involved to carry out the inverse transformation for higher orders. For example, the solution of the twelfth order of the NZ equation as obtained by standard computer algebra tools is filling some hundred pages, whereas the solution of the TCL equation can be written in a single line.

The solutions of the master equations in second and fourth order are plotted in Figs. 4 and 5, together with the

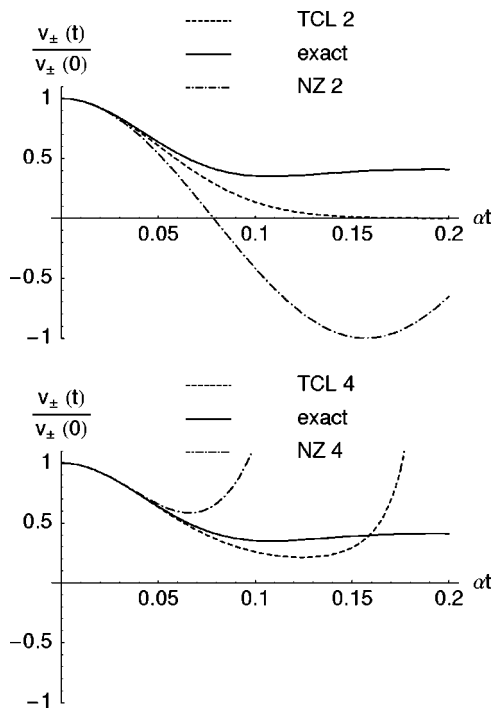


FIG. 4. Comparison of the TCL and the NZ technique with the exact solution. The plot shows the approximations to second and fourth order in α and the exact solution of $v_{\pm}(t)$ [see Eqs. (23) and (28)] for a bath of 100 spins.

exact solutions. We observe that both methods lead to a good approximation of the short-time behavior of the components of the Bloch vector. We further see that the TCL technique is not only easier to solve, but also provides a better approximation of the dynamics within a given order.

Since the TCL and the NZ method lead to expansions of the equations of motion and not of their solutions, the solutions of the truncated equations may contain terms of arbitrary order in the coupling strength. For example, even though TCL2 is a second-order approximation, the corresponding solution given by Eqs. (48) and (49) contains infinitely many orders. Of course, the expansion of the exact solution coincides with the expansion of the approximations obtained with $TCL2n$ or $NZ2n$ within the $(2n)$ th order. The error of TCL2 or NZ2, for example, is therefore a term of order α^4 , as is illustrated in Fig. 6.

Concerning the long-time behavior, both the TCL and the NZ methods may lead to very bad approximations. For example, in the fourth-order approximation of $v_{\pm}(t)$ (see Fig. 4) the TCL as well as the NZ solution leave the Bloch sphere, i.e., for times larger than some critical time these solutions do not represent true density matrices anymore.

If we look at higher orders, the NZ method is seen to be better than the TCL method as far as the three-component of the Bloch vector is concerned. An example is shown in Fig. 7, where we plot the tenth-order approximations. We observe that the solution $v_3(t)$ of the TCL equation (58) is always greater than zero. This fact is obviously connected to the structure of this equation, which takes the form $\dot{v}_3(t) = \mathcal{K}_3(t)v_3(t)$ with a real function $\mathcal{K}_3(t)$. If the three-component v_3 of the Bloch vector vanishes at the time $t=t_0$,

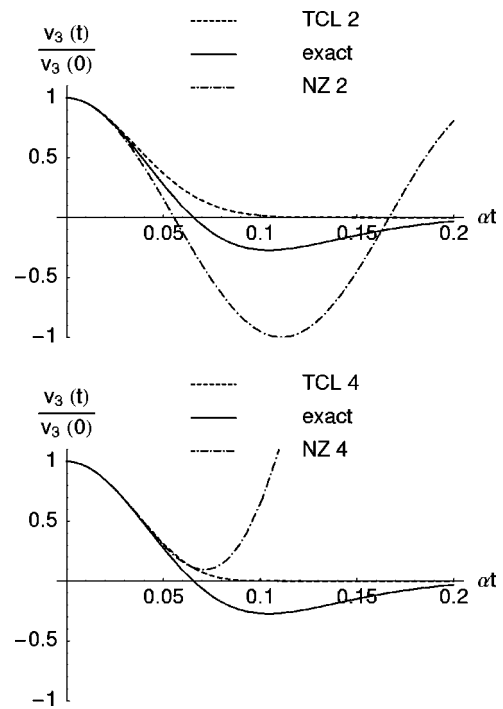


FIG. 5. Comparison of the TCL and the NZ technique with the exact solution. The plot shows the second- and the fourth-order approximations as well as the exact solution of $v_3(t)$ [see Eqs. (24) and (29)] for a bath of 100 spins.

then a time-local equation of motion of this form can only be fulfilled if $\dot{v}_3(t_0)$ is also zero. In our case, however, the exact solution passes zero with a nonvanishing time derivative. It is a well-known fact⁸ that the perturbation expansion of the TCL generator only exists, in general, for short and intermediate times and /or coupling strengths. This is reflected in the fact that the superoperator on the right-hand side of Eq. (32) cannot be inverted for all times, i.e., it is not always possible to express $v_3(0)$ in terms of $v_3(t)$. A similar situation also occurs in open systems interacting with a bosonic reservoir, e.g., in the damped Jaynes Cummings model which describes the interaction of a qubit with a bosonic reservoir at zero temperature. The NZ technique does not lead to such problems. However, since the components $v_{\pm}(t)$ do not vanish, the corresponding high-order TCL approximation is still

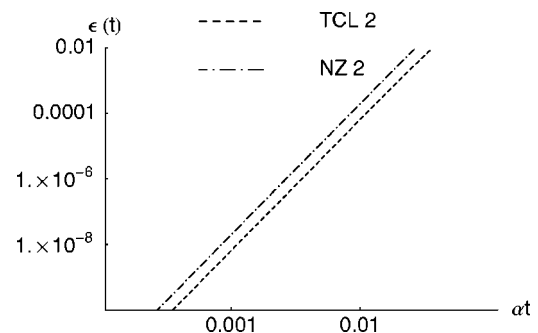


FIG. 6. Error of TCL2 and NZ2: The plot shows the deviation $\epsilon(t) \equiv |v_{\pm}(t) - v_{\pm}^{\text{approx}}(t)|$ of the exact solution $v_{\pm}(t)$ from the approximate solution $v_{\pm}^{\text{approx}}(t)$ for small αt .

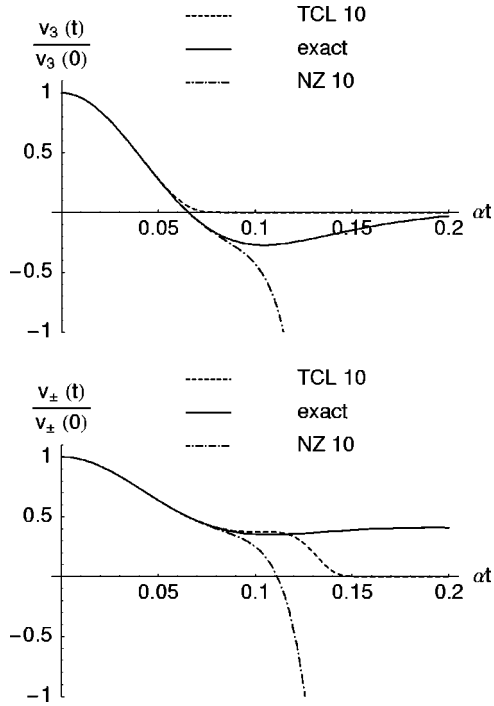


FIG. 7. The TCL and the NZ approximation of the components of the Bloch vector in tenth order for a bath of 100 spins.

more accurate than the NZ approximation, as may be seen from Fig. 7.

IV. CONCLUSION

With the help of a simple analytically solvable model of a spin star system, we have discussed the performance of projection operator techniques for the dynamics of open systems and the resulting perturbation expansions of the equations of motion. The model consists of a central spin surrounded by a bath of spins interacting with the central spin through a Heisenberg XY coupling, and shows complete relaxation and partial decoherence in the limit of an infinite number of bath spins. Due to its high symmetry the model allows a direct comparison of the Nakajima-Zwanzig (NZ) and of the time-convolutionless (TCL) projection operator methods with the exact solution in analytical terms.

While the Born-Markov limit of the equation of motion does not exist in the model, the dynamics of the central spin exhibits a pronounced non-Markovian behavior. It has been demonstrated that both the NZ and the TCL techniques provide good approximations of the short-time dynamics. In practical applications the TCL method is usually to be preferred since it leads to time-local equations of motion in any desired order with a much easier mathematical structure, whose integration is much simpler than that of the nonlocal equations of the NZ technique.

It should be kept in mind, however, that the expansion based on the TCL method converges, in general, only for short and intermediate interaction times. For large times the perturbation expansion may break down, which has been illustrated in our model to be connected to zeros of the com-

ponents of the Bloch vector. It turns out that the NZ equation of motion yields a better approximation of the exact dynamics in this regime.

In view of the heuristic approach to the Born and to the Redfield equation (see Sec. III A) it is sometimes conjectured that a nonlocal equation of motion should be generally better than a time-local one. The results of Sec. III B show that this conjecture is, in general, not true. The fact that in a given order the time-local TCL equation is at least as good (and much simpler to deal with), if not better than the nonlocal NZ equation has also been observed in other specific system-reservoir models⁸ and has been confirmed by general mathematical arguments.³⁷ However, care must be taken when applying a certain projection operator method to a specific model: The quality of the corresponding perturbation expansion of the equation of motion may strongly depend on the specific properties of the model, e.g., the interaction Hamiltonian, the interaction time, the environmental state and the spectral density.

For example, in our particular model the TCL expansion to fourth order turns out to be more accurate than the fourth-order NZ expansion. However, there is no reason why TCL should be generally better than NZ. To clarify further this point we consider the Taylor series of the three-component of the Bloch vector:

$$v_3(t) = a_0 + a_2(at)^2 + a_4(at)^4 + O((at)^6). \quad (61)$$

The corresponding expansion obtained from TCL2 is given by

$$v_3(t) = a_0 + a_2(at)^2 + \frac{a_2^2}{2a_0}(at)^4 + O((at)^6), \quad (62)$$

while NZ2 gives the expansion

$$v_3(t) = a_0 + a_2(at)^2 + \frac{a_2^2}{6a_0}(at)^4 + O((at)^6). \quad (63)$$

In our model the exact coefficients of the expansion (61) are found to be

$$a_0 = 1, \quad a_2 = -4N, \quad a_4 = \frac{16}{3}N^2. \quad (64)$$

Of course, the second order coefficient a_2 is the same in all expansions, while in general neither TCL2 nor NZ2 reproduce correctly the fourth order coefficient a_4 . However, in our model it turns out that the TCL2 approximation is more accurate because the fourth order coefficient

$$\frac{a_2^2}{2a_0} = \frac{16}{2}N^2 \quad (65)$$

found from the solution of the TCL equation is closer to the correct fourth-order coefficient a_4 than the corresponding coefficient

$$\frac{a_2^2}{6a_0} = \frac{16}{6}N^2 \quad (66)$$

of the NZ equation (see Fig. 6). Thus we see that it depends crucially on the value of a_4 whether TCL2 or NZ2 is better.

Choosing an appropriate interaction Hamiltonian and initial state, one can easily construct examples where NZ2 is better than TCL2. For example, if $v_3(t)$ was a cosine function $a_0 \cos(\alpha t)$, then NZ2 would already give the exact solution. On the other hand, if $v_3(t)$ was a Gaussian function $a_0 \exp(-\alpha^2 t^2)$, then TCL2 would reproduce the exact solution because the higher cumulants of a Gaussian function vanish.

The features discussed above should be taken into account in applications of projection operator methods to specific open systems. In the general case in which an analytical solution is not known a careful analytical or numerical investigation of the higher orders of the respective expansions is thus indispensable to judge the quality of the TCL or the NZ method, the influence of initial correlations, or to estimate the time scale over which one can trust the approximation obtained within a given order.

APPENDIX: BATH CORRELATION FUNCTIONS

In this appendix we outline how to calculate the bath correlation functions

$$Q_k \equiv \frac{1}{2^N} \text{tr}_B \{ (J_+ J_-)^k \}, \quad (\text{A1})$$

$$R_l^{k-l} \equiv \frac{1}{2^N} \text{tr}_B \{ (J_+ J_-)^{k-l} (J_- J_+)^l \}. \quad (\text{A2})$$

The trace can be computed in the eigenbasis of J_3 and \mathbf{J}^2 (see Sec. II B) yielding a sum of polynomials in j and m . However, it turns out that it is easier to use the computational basis of the spin bath consisting of the states

$$|s_1\rangle \otimes |s_2\rangle \otimes \cdots \otimes |s_N\rangle, \quad (\text{A3})$$

where the s_i take on the values 0 or 1 and

$$\sigma_3^{(i)} |s_i\rangle = (-1)^{s_i} |s_i\rangle. \quad (\text{A4})$$

With the help of these states the problem is reduced to a combinatorial one. Since

$$J_{\pm} = \sum_{i=1}^N \sigma_{\pm}^{(i)} \quad (\text{A5})$$

we have

$$(J_+ J_-)^k = \sum_{i_1, \dots, i_{2k}} \sigma_+^{(i_1)} \sigma_-^{(i_2)} \sigma_+^{(i_3)} \sigma_-^{(i_4)} \dots \sigma_+^{(i_{2k-1})} \sigma_-^{(i_{2k})}, \quad (\text{A6})$$

where the summation is taken over all possible combinations of the indices i_1, i_2, \dots, i_{2k} . Under the trace over the bath we can sort these indices, without interchanging the operators belonging to the same index, and calculate the partial traces over the various bath spins separately.

Let us denote the partial trace over the Hilbert space of the i th bath spin by tr_i . For example, we have for $k=2$:

$$\text{tr}_B \{ \sigma_+^{(1)} \sigma_-^{(3)} \sigma_+^{(4)} \sigma_-^{(1)} \} = \text{tr}_1 \{ \sigma_+^{(1)} \sigma_-^{(1)} \} \text{tr}_3 \{ \sigma_-^{(3)} \} \text{tr}_4 \{ \sigma_+^{(4)} \} 2^{N-3} = 0, \quad (\text{A7})$$

since $\text{tr}_i \{ \sigma_{\pm}^{(i)} \} = 0$. Note that the factor 2^{N-3} appears due to $(N-3)$ factors of $\text{tr}_i \{ I \} = 2$. These factors arise from the partial

traces of the unit matrices I in the spin spaces, which we did not write explicitly. As a further example, we have for $k=4$:

$$\begin{aligned} \text{tr}_B \{ \sigma_+^{(1)} \sigma_-^{(3)} \sigma_+^{(1)} \sigma_-^{(1)} \sigma_+^{(3)} \sigma_-^{(1)} \} \\ = \text{tr}_1 \{ \sigma_+^{(1)} \sigma_+^{(1)} \sigma_-^{(1)} \sigma_-^{(1)} \} \text{tr}_3 \{ \sigma_-^{(3)} \sigma_+^{(3)} \} 2^{N-2} = 0, \end{aligned} \quad (\text{A8})$$

because of $\sigma_{\pm}^{(i)} \sigma_{\pm}^{(i)} = 0$. An example of a nonvanishing term is given by

$$\text{tr}_B \{ \sigma_+^{(1)} \sigma_-^{(2)} \sigma_+^{(2)} \sigma_-^{(1)} \} = \text{tr}_1 \{ \sigma_+^{(1)} \sigma_-^{(1)} \} \text{tr}_2 \{ \sigma_-^{(2)} \sigma_+^{(2)} \} 2^{N-2} = 2^{N-2}, \quad (\text{A9})$$

where we have used the fact that $\text{tr}_i \{ \sigma_{\pm}^{(i)} \sigma_{\pm}^{(i)} \} = 1$.

In view of these considerations we are now left with the combinatorial problem of determining all nonzero summands for the given values of k and l . As an example, let us calculate explicitly the correlation function Q_2 . From its definition we have

$$Q_2 = \frac{1}{2^N} \text{tr}_B \{ J_+ J_- J_+ J_- \} = \frac{1}{2^N} \sum_{i_1, i_2, i_3, i_4} \text{tr}_B \{ \sigma_+^{(i_1)} \sigma_-^{(i_2)} \sigma_-^{(i_3)} \sigma_+^{(i_4)} \}. \quad (\text{A10})$$

The nonzero summands in this expression have the following structure:

$$\sigma_+^{(i)} \sigma_-^{(i)} \sigma_+^{(i)} \sigma_-^{(i)} \rightarrow N \text{ possibilities,}$$

$$\sigma_+^{(i)} \sigma_-^{(i)} \sigma_+^{(j)} \sigma_-^{(j)} \rightarrow N(N-1) \text{ possibilities,}$$

$$\sigma_+^{(i)} \sigma_-^{(j)} \sigma_+^{(j)} \sigma_-^{(i)} \rightarrow N(N-1) \text{ possibilities,}$$

where $i \neq j$ in the second and the third line. Collecting these results we find

$$Q_2 = \frac{1}{2^N} [N \times 2^{N-1} + 2N(N-1) \times 2^{N-2}] = \frac{N^2}{2}. \quad (\text{A11})$$

A similar procedure must be carried out to calculate R_l^{k-l} . We state some results:

$$Q_3 = \frac{1}{2} N - \frac{3}{4} N^2 + \frac{3}{4} N^3,$$

$$Q_4 = -2N + 5N^2 - 4N^3 + \frac{3}{2} N^4,$$

...

$$R_1^1 = -\frac{1}{2} N + \frac{1}{2} N^2,$$

$$R_2^1 = \frac{1}{2} N - \frac{5}{4} N^2 + \frac{3}{4} N^3,$$

$$R_3^1 = -\frac{5}{2} N + \frac{23}{4} N^2 - \frac{19}{4} N^3 + \frac{3}{2} N^4,$$

...

It should be clear that the above method of determining the correlation functions is easily translated into a numerical

code from which one obtains the Q_k and the R_l^{k-l} in any desired order.

For $N \geq k$, the term of leading order in N of the polynomials Q_k and R_l^{k-l} is represented by the summands with a maximal number of k different indices, because these terms have the largest combinatorial weight. After sorting the spin operators, these terms will have the following form,

$$\sigma_+^{(i_1)} \sigma_-^{(i_1)} \sigma_+^{(i_2)} \sigma_-^{(i_2)} \dots \sigma_+^{(i_k)} \sigma_-^{(i_k)}. \quad (\text{A12})$$

There are $\binom{N}{k}$ different ways of assigning the indices i_1, i_2, \dots, i_k to this term. For a fixed set of indices, there are $k! \cdot k!$ different terms in the sum (A6) which lead to the sorted expression (A12), corresponding to a permutation of

the labels of all σ_+ operators and of all σ_- operators. The trace of the expression (A12) yields 2^{N-k} . Hence, the term of leading order of the polynomial Q_k is found to be

$$2^{-N} \binom{N}{k} k! \cdot k! 2^{N-k} \approx \frac{N^k k!}{2^k}. \quad (\text{A13})$$

A similar proof holds for R_l^{k-l} . Thus, we have for $N \rightarrow \infty$ and k fixed:

$$Q_k \approx R_l^{k-l} \approx \frac{k!}{2^k} N^k, \quad (\text{A14})$$

which has been used in Sec. II C.

-
- ¹M. A. Nielsen and I. L. Chuang, *Quantum Computation and Quantum Information* (Cambridge University Press, Cambridge, 2000).
- ²D. Loss and D. P. DiVincenzo, Phys. Rev. A **57**, 120 (1998).
- ³B. E. Kane, Nature (London) **393**, 133 (1998).
- ⁴D. D. Awschalom, N. Samarth, and D. Loss, *Semiconductor Spintronics and Quantum Computation* (Springer, New York, 2002).
- ⁵S. Bose, Phys. Rev. Lett. **91**, 207901 (2003).
- ⁶J. I. Cirac and P. Zoller, Phys. Rev. Lett. **74**, 4091 (1995).
- ⁷T. Pellizzari, S. A. Gardiner, J. I. Cirac, and P. Zoller, Phys. Rev. Lett. **75**, 3788 (1995).
- ⁸H.-P. Breuer and F. Petruccione, *The Theory of Open Quantum Systems* (Oxford University Press, Oxford, 2002).
- ⁹A. Khaetskii, D. Loss, and L. Glazman, Phys. Rev. B **67**, 195329 (2003).
- ¹⁰D. Mozyrsky, Nano Lett. **2**, 651 (2002).
- ¹¹R. de Sousa and S. Das Sarma, Phys. Rev. B **68**, 115322 (2003).
- ¹²D. Mozyrsky, Lett. Math. Phys. **55**, 1 (2001).
- ¹³M. Frasca, J. Opt. B: Quantum Semiclassical Opt. **4**, S443 (2002).
- ¹⁴N. Makri, J. Chem. Phys. **111**, 6164 (1999).
- ¹⁵N. Makri, J. Phys. Chem. **103**, 2823 (1999).
- ¹⁶K. M. Forsythe and N. Makri, Phys. Rev. B **60**, 972 (1999).
- ¹⁷J. Shao and P. Hänggi, Phys. Rev. Lett. **81**, 5710 (1998).
- ¹⁸J. Schliemann, A. Khaetskii, and D. Loss, J. Phys.: Condens. Matter **15**, R1809 (2003).
- ¹⁹N. V. Prokof'ev and P. C. E. Stamp, Rep. Prog. Phys. **63**, 669 (2000).
- ²⁰C. Cohen-Tannoudji, J. Dupont-Roc, and G. Grynberg, *Atom-Photon Interactions* (Wiley, New York, 1998).
- ²¹C. W. Gardiner and P. Zoller, *Quantum Noise* (Springer, New York, 2000).
- ²²S. Nakajima, Prog. Theor. Phys. **20**, 948 (1958).
- ²³R. Zwanzig, J. Chem. Phys. **33**, 1338 (1960).
- ²⁴H. Mori, Prog. Theor. Phys. **33**, 423 (1965).
- ²⁵F. Shibata and T. Arimitsu, J. Phys. Soc. Jpn. **49**, 891 (1980).
- ²⁶A. Royer, Phys. Rev. A **6**, 1741 (1972).
- ²⁷N. G. v. Kampen, Physica (Amsterdam) **74**, 239 (1974).
- ²⁸N. G. v. Kampen, Physica (Amsterdam) **74**, 215 (1974).
- ²⁹A. Hutton and S. Bose, Phys. Rev. A **69**, 042312 (2004).
- ³⁰E. H. Lieb, T. D. Schultz, and D. C. Mattis, Ann. Phys. (N.Y.) **16**, 407 (1961).
- ³¹A. Imamoglu, D. D. Awschalom, G. Burkard, D. P. DiVincenzo, D. Loss, M. Sherwin, and A. Small, Phys. Rev. Lett. **83**, 4204 (1999).
- ³²S.-B. Zheng and G.-C. Guo, Phys. Rev. Lett. **85**, 2392 (2000).
- ³³V. Privman, I. D. Vagner, and G. Kventsel, Phys. Lett. A **239**, 141 (1998).
- ³⁴A. Sørensen and K. Mølmer, Phys. Rev. Lett. **83**, 2274 (1999).
- ³⁵J. Wesenberg and K. Mølmer, Phys. Rev. A **65**, 062304 (2002).
- ³⁶K. Hepp and E. H. Lieb, Helv. Phys. Acta **46**, 573 (1976).
- ³⁷A. Royer, Phys. Lett. A **315**, 335 (2003).